Chiral nodes and oscillations in the Josephson current in Weyl semimetals

Udit Khanna, Dibya Kanti Mukherjee, Arijit Kundu, and Sumathi Rao

Chiral nodes and oscillations in the Josephson current in Weyl semimetals

Udit Khanna,[1] Dibya Kanti Mukherjee,[1] Arijit Kundu,[2, 3] and Sumathi Rao[1]

[1]*Harish-Chandra Research Institute, Chhatnag Road, Jhunsi, Allahabad 211 019, India.*
[2]*Physics Department, Technion, 320003, Haifa, Israel*
[3]*Department of Physics, Indiana University, Bloomington, IN 47405*

The separation of the Weyl nodes in a broken time-reversal symmetric Weyl semimetal leads to helical quasi-particle excitations at the Weyl nodes, which, when coupled with overall spin conservation allows only inter-nodal transport at the junction of the Weyl semimetal with a superconductor. This leads to an unusual periodic oscillation in the Josephson current as a function of $k_0 L$, where L is the length of the Weyl semimetal and $2k_0$ is the inter-nodal distance. This oscillation is robust and should be experimentally measurable, providing a direct path to confirming the existence of chiral nodes in the Weyl semimetal.

Introduction.—Weyl semimetals (WSM), which have received much interest recently due to their non-trivial transport characteristics, are 3D topological systems where conduction and valence bands touch at two or more 'Weyl' points[1–5]. According to a no-go theorem[6], gapless Weyl nodes in a WSM appear as pairs in momentum space with each of the nodes having a definite 'chirality', a quantum number that depends on the Berry flux enclosed by a closed surface around the node. Gauss law prevents the annihilation of the nodes unless two of them with opposite chirality are brought together, which provides the 'topological' protection of the Weyl nodes[7]. A WSM phase requires broken time-reversal and/or inversion symmetry and a growing number of systems has been put forward which realize the WSM phase[8–10].

The separation of the chiral nodes, allows charge pumping between the nodes in the presence of parallel electric and magnetic fields, as a consequence of the chiral anomaly[11], and this has led to detailed studies of transport in Weyl semi-metals in several recent papers[12–32].

In this paper we study the current in a simple Josephson junction setup, depicted in Fig. 1(a). The helical quasi-particle excitations at the Weyl nodes, due to the overall spin conserving processes at a WSM-superconductor (SC) junction, allow only inter-nodal transport[33]. Further, we show, unlike in a normal metal-SC interface, the inter-nodal 'normal' (electron to electron) reflection process in a WSM-SC interface is not suppressed even for energies close to Fermi-energy, due to the broken time-reversal symmetry separating the Weyl nodes. The Josephson current, flowing through the bound levels formed by multiple inter-nodal 'normal' and Andreev (electron to hole) processes in a SC-WSM-SC system, consequently, acquires a specific periodicity as a function of the length of the WSM which depends only on the separation of the Weyl nodes in the momentum space (see Fig. 1(b)). We argue that both of these features are robust because they are not only bulk effects, but they are also protected by the robustness of the Weyl nodes. We also discuss the feasibility of experimental observations of this transition in our system, which can confirm the presence of chiral nodes in WSM.
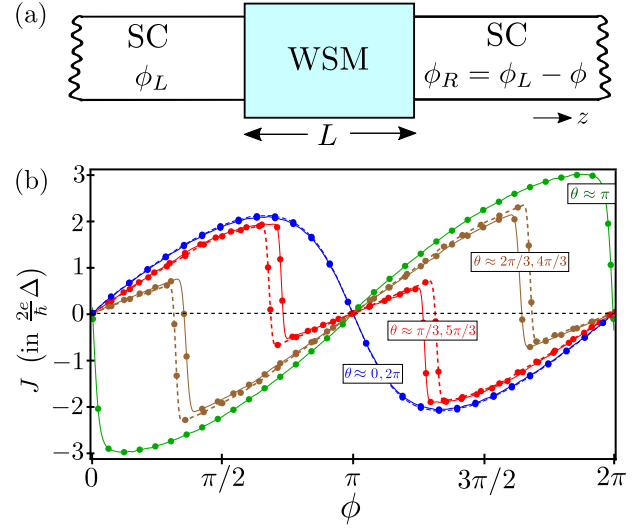

FIG. 1. (Color online) (a) The setup for Josephson current with two superconductors (SC) characterized by phases ϕ_L and ϕ_R sandwiching a WSM of length L between them where a time-reversal broken perturbation separates the Weyl nodes in momentum space by $2k_0$ in k_z. (b) The Josephson current (at normal incidence) is periodic in L with a period of π/k_0. We show the zero-temperature Josephson current, Eq. (9), as a function of the superconducting phase difference ϕ, for various values of L in solid (dashed) lines for θ between 0 and π (π and 2π), where $\theta = 2k_0 L \bmod(2\pi)$. The parameters used are $k_0 L = 31.4, 32.0, 32.5, 33, 33.5, 34.0, 34.454$, $\hbar^2 k_0^2/2m_W = 10\mu_W = 10^3\Delta = \mu_S/2$, $p \ll k_0$ and $m_S = m_W$.

This oscillation in the Josephson current and the resulting changes of sign of the critical current at arbitrary values of ϕ (or the 0-π transition) is an inherent property of the SC-ferromagnet-SC junction[34–37] and has also been experimentally observed[38]. Since our model also explicitly violates time-reversal invariance, our results show quite a strong similarity with the Josephson current in similar systems[39] as well in semiconductor nanowires with Zeeman coupling[40].

Model and geometry.—We consider the geometry as shown in Fig. 1(a) with the superconductors at $z < 0$

and $z > L$ and the Weyl semimetal (WSM) in the region $0 < z < L$. We model the WSM starting from the standard Hamiltonian describing a 3D TI in the Bi_2Se_3 family[41,42], regularized on a simple cubic lattice and adding a time-reversal breaking perturbation b_z to access the WSM phase[19] -

$$H_0 = \epsilon_k \tau_x - \lambda_z \sin k_z \tau_y$$
$$- \lambda \tau_z (\sigma_x \sin k_y - \sigma_y \sin k_x) + b_z \sigma_z. \quad (1)$$

Here $\epsilon_k = \epsilon - 2t \sum_i \cos k_i$ is the kinetic energy, τ (σ) represent the orbital (spin) degrees of freedom and λ, λ_z are the strengths of the spin-orbit coupling. In the limit $\lambda_z \ll M \ll b_z$, (where M is defined as $\epsilon - 6t$[43]), this simplifies to a two-band model for a WSM, where, in the absence of the spin-orbit coupling, λ, the bands have opposite spins[33,43]. The chiral fermion excitations around the two Weyl nodes (which we choose to be at $(0, 0, \pm k_0)$, where $tk_0^2 = b_z - M$) are described by the Hamiltonian

$$H_{WSM} = \epsilon_k \sigma_z - \mu_W + \lambda(k_x \sigma_x + k_y \sigma_y) \quad (2)$$

with $\epsilon_k = (\hbar^2/2m_W)(k_x^2 + k_y^2 + k_z^2 - k_0^2)$ being the kinetic energy, μ_W being the chemical potential measured from the Weyl node and m_W being the effective mass. Since the Weyl nature of the fermions is only evident at momenta which are small with respect to the symmetry breaking scale k_0, we choose the Fermi energy μ_W to be small enough, so that the Fermi surfaces around the two Weyl nodes are disconnected. The surface states for this model appear on the surfaces perpendicular to the x-axis and y-axis. In this paper, we do not attempt to access transport through the surface states. Instead, we consider transport through the bulk of the WSM and hence restrict ourselves to transport parallel to the z-axis.

The superconductors can be described in terms of the Boguliobov-de Gennes (BdG) Hamiltonian as

$$H_{SC}^j = \begin{pmatrix} \xi_k I_{2\times2} & e^{i\phi_j}\Delta i\sigma_y \\ -e^{-i\phi_j}\Delta i\sigma_y & -\xi_k I_{2\times2} \end{pmatrix}, \quad (3)$$

where Δ is the pairing potential in the superconductor and $\xi_k = (\hbar^2(k_x^2 + k_y^2 + k_z^2)/2m_S - \mu_S)$. m_S is the effective mass of the electron in the superconductor and μ_S is the chemical potential. ϕ_j is the superconducting phase of the jth superconductor. For the left and right superconductors, $j = L, R$. The parameter μ_S depends on the details of the superconducting material. In the numerical results shown, we consider $\mu_S \gg \Delta$, which is the realistic limit. Also, for simplicity, we consider $m_S \approx m_W$.

WSM-SC junction.—The solutions of Eq. (2) in the Nambu-Gor'kov space are now 4 component spinors. For incident energy E, the right-moving solutions with the wavefunctions proportional to $e^{\nu i k_e^\nu z}$ for electrons and $e^{-\nu i k_h^\nu z}$ for holes can be written in the basis of the two bands $\nu = \pm$, with

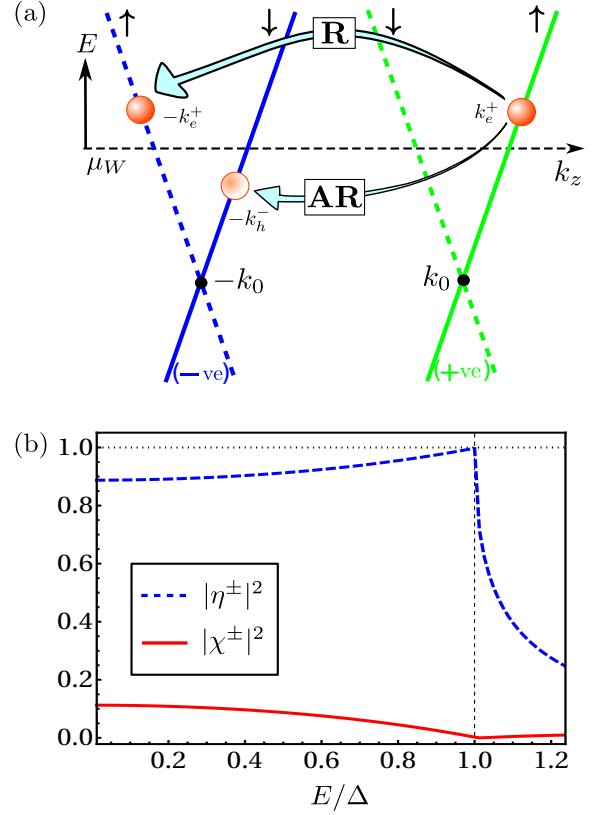$$k_{e(h)}^\nu = \sqrt{k_0^2 - p^2 + \nu(2m_w/\hbar^2)\sqrt{(\mu_W + (-)E)^2 - (\lambda p)^2}}$$

FIG. 2. (Color online) (a) Both reflection (R) and Andreev reflection (AR) in WSM occur from one chiral node to another. The chiralities of the nodes are denoted as +ve and −ve, whereas the solid and the dashed lines show dispersions of Eq. (2) with positive and negative velocities (= dE/dk). The bands have opposite spins, which accounts for the change of chirality for both 'normal' and Andreev reflection. (b) The probability that an electron will be reflected as an electron ($|\chi^\pm|^2$) or as a hole ($|\eta^\pm|^2$) at a WSM-SC interface, discussed in Eq. (5). Note that the probability of reflection as an electron is finite. The parameters used are the same as in Fig. 1(b).

and $p = \sqrt{k_x^2 + k_y^2}$. The left-moving solutions can be written similarly with $k_{e(h)}^\nu \rightarrow -k_{e(h)}^\nu$. For the case of a WSM-SC junction, the WSM and and the superconducting wavefunctions on the two sides of the junction can be matched at the junction by requiring the continuity of the wavefunction and its first derivative[43]. This leads to the net reflection matrix $\mathcal{R}^j$ from the WSM-SC junction, which connects the left and right-moving solutions,

$$\mathcal{R}^j = \begin{pmatrix} r_{ee}^j & r_{eh}^j \\ r_{he}^j & r_{hh}^j \end{pmatrix}, \quad (4)$$

where the 'normal' reflection matrices $r_{ee}^j(r_{hh}^j)$, and the Andreev reflection matrices $r_{eh}^j(r_{he}^j)$ denote, respectively, electron to electron (hole to hole) and hole to electron (electron to hole) processes at the interface with the jth superconductor.
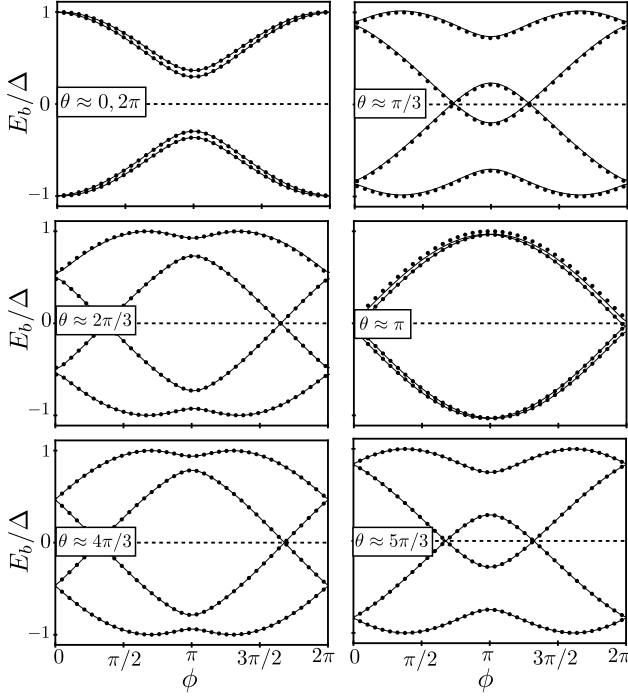
FIG. 3. The variation of the bound levels (solutions of Eq. (6)) near the chemical potential with the length L of the WSM for various values of θ, where $\theta = 2k_0L \bmod(2\pi)$. The parameters used are the same as in Fig. 1(b).

For the purpose of physical interpretation, let us take the case of near-normal incidence ($k_0 \gg p$) of an electron, where the reflection matrices reduce to the form:

$$r_{ee}^{j} = \begin{pmatrix} \chi^+ & 0 \\ 0 & \chi^- \end{pmatrix}, \quad r_{he}^{j} = e^{-i\phi_j} \begin{pmatrix} 0 & \eta^+ \\ \eta^- & 0 \end{pmatrix}. \quad (5)$$

In this simplified form it is immediately clear that both the reflection and the Andreev reflection change the chirality (see also Fig. 2(a)) and can only take place from one node to another because of the chiral nature of the nodes. We plot the probabilities of normal and the Andreev reflection in Fig. 2(b). We note that even at energies close to the Fermi energy, normal reflection is not suppressed. The existence of the new momentum scale $k_0 \neq k_F$, introduced by breaking the time-reversal symmetry, allows the incident electron momentum to be different from the Fermi momentum of the superconductor. This leads to the non vanishing of normal reflection[43,44]

In contrast, note that for a topological insulator in 3D, the bulk is gapped and the non-trivial transport in junctions with superconductors is purely due to the surface states, where, the surface states consist of a Dirac metal with an odd number of nodes whose fermions have their spins aligned with the direction of motion (spin-momentum locking). This leads to completely different physics for a topological insulator-superconductor junction[45,46]. Two dimensional graphene, on the other hand, is metallic and the transport is through the bulk. However, in graphene, although there are two Dirac nodes
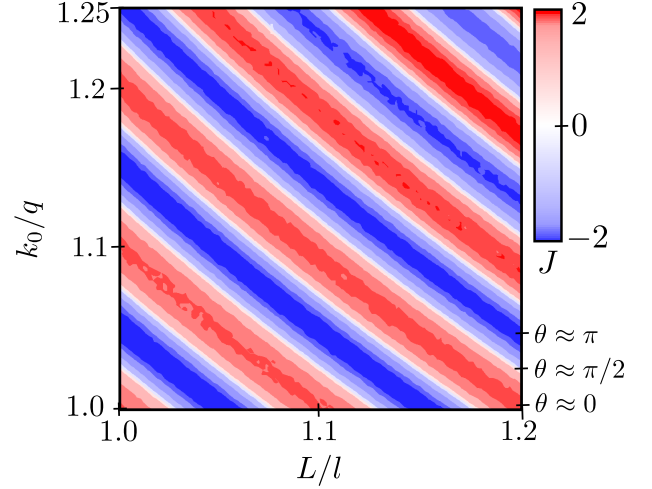

FIG. 4. (Color online) The Josephson current as a function of both L and k_0 is shown at the value of $\phi \approx \pi/2$. The initial value at the origin is $(k_0, L) = (q, l)$, $ql \approx 10\pi$. The contours of constant current follow a set of (approximate) hyperbolas for constant $\theta = 2k_0L \bmod(2\pi)$, a few of which are shown in the right margin (with the minimum and the maximum current occuring near $\theta = \pi$ and $\theta = 0$ respectively). Other parameters used are the same as in Fig. 1(b).

(valleys), each of the nodes has fermions of both chiralities and the resulting process at the a superconducting interface is purely intra-nodal Andreev reflection[47,48].

Bound levels in the SC-WSM-SC geometry.—Multiple reflections at the *WSM-SC* boundaries lead to bound electronic levels in the *SC-WSM-SC* geometry. But as discussed above, normal reflection amplitudes are not small at the *WSM-SC* interface and, in general, there is no simple way of summing up the amplitudes between the two superconductors to obtain the resonance condition when both Andreev and normal reflection amplitudes are non-zero. For the case of near normal incidence, however, the problem simplifies and the bound levels E_b can be found by solving

$$\det \left[I_{4\times4} - \mathcal{R}^L \mathcal{M} \mathcal{R}^R \mathcal{M} \right] \big|_{E=E_b} = 0, \quad (6)$$

where $\mathcal{M}$ is the matrix which accounts for the phase the electron/hole acquires while moving from one junction to another. We note that for $k_0 \gg p$, Eq. (6) can still be used for approximate solutions. Writing

$$\mathcal{R}^L \mathcal{M} \mathcal{R}^R \mathcal{M} = \begin{pmatrix} \mathcal{T}_{ee} & \mathcal{T}_{eh} \\ \mathcal{T}_{he} & \mathcal{T}_{hh} \end{pmatrix}, \quad (7)$$

in the limit of near normal incidence with $k_0^2/2m_W$ much larger than incident energy E and μ_S much larger than pairing potential Δ, the $\mathcal{T}$ matrices have the simplified

form (with $m_S = m_W$):[43]

$$\mathcal{T}_{ee} = \begin{pmatrix} \alpha^+ & 0 \\ 0 & \alpha^- \end{pmatrix}, \quad \mathcal{T}_{he} = \begin{pmatrix} 0 & \beta^+ \\ \beta^- & 0 \end{pmatrix}, \quad (8)$$

with $\quad \alpha^\pm \approx e^{\pm 2ik_0 L}(1 + 4iE\delta)$,

$$\beta^\pm \approx \pm e^{\mp 2ik_0 L} 2i(1 + e^{-i\phi})\Delta,$$

where $\delta = \sqrt{2m_W\mu_S}/k_0\Omega$ and $\phi = \phi_R - \phi_L$,. Also $\mathcal{T}_{hh} = \mathcal{T}_{ee}^*(E \to -E)$, $\mathcal{T}_{eh} = \mathcal{T}_{he}^*(E \to -E)$. This immediately shows the periodicities of the $\mathcal{T}$ matrices, $\mathcal{T}(\phi) = \mathcal{T}(\phi \to \phi + 2\pi)$ and $\mathcal{T}(2k_0 L) = \mathcal{T}(2k_0 L \to 2k_0 L + 2\pi)$, which implies that the bound levels E_b, the solutions of Eq. 6, also inherit the same periodicities in ϕ and $2k_0 L$. This additional periodicity of the levels with period (π/k_0) in length appears as a consequence of the inter-nodal normal and the Andreev reflections. The periodicities of E_b in the difference of the superconducting phases ϕ and in $2k_0 L$, in the limit of $k_0 \gg p$ is shown in Fig. 3. This is our central result.

Periodic oscillations in the Josephson current.—The Josephson current for the system with the total Hamiltonian H is written as $J_{\text{jos}} = \frac{2e}{\hbar}\left\langle \frac{\partial H}{\partial \phi} \right\rangle$, where the average is taken over the states of the system. For the non-interacting system, where the length L is much smaller than the coherence length in superconductors, the Josephson current flows through the bound levels (neglecting the continuum contribution) and can be estimated as[49]

$$J(\mu_W) = \frac{2e}{\hbar}\sum_b \frac{\partial E_b}{\partial \phi} f(E_b - \mu_W), \quad (9)$$

where f is the Fermi-distribution function. Apart from the 2π periodicity of the Josephson current in ϕ, as the bound levels E_b are periodic in L with the periodicity of π/k_0, the Josephson current also inherits the same periodicity. This periodicity is shown explicitly in Fig. 1(b) for the case when $p = 0$.

The periodic dependence in L can also be written as an approximate periodicity in k_0 with a period of π/L. For large values of L, the rapid oscillations of E_b with a small variation of k_0 outweighs any other dependence on k_0 and the periodicity is almost exact. The Josephson current as a function of both k_0 and L is also shown in Fig. 4, where the locus of constant current approximately follows $\theta = 2k_0 L \bmod(2\pi)$. This is another of our main results.

Lattice simulation.—To analyse the case for non-normal incident angle $p \neq 0$, we compute the Josephson current from the lattice version of Eq. (1) through its Green's function[43,50]. The Green's function of the WSM, $g(\omega) = [(\omega + i\delta)\mathcal{I} - H_0]^{-1}$, is coupled with two superconductors $i = L, R$ through the on-site self energy[19]

$$\Sigma_i(\omega) = \frac{\tilde{t}}{\sqrt{\Delta^2 - \omega^2}}(\mathcal{I}_\tau + \tau^x)[\omega\mathcal{I}_\zeta - \Delta e^{i\phi_i}\zeta^x]\mathcal{I}_\sigma. \quad (10)$$
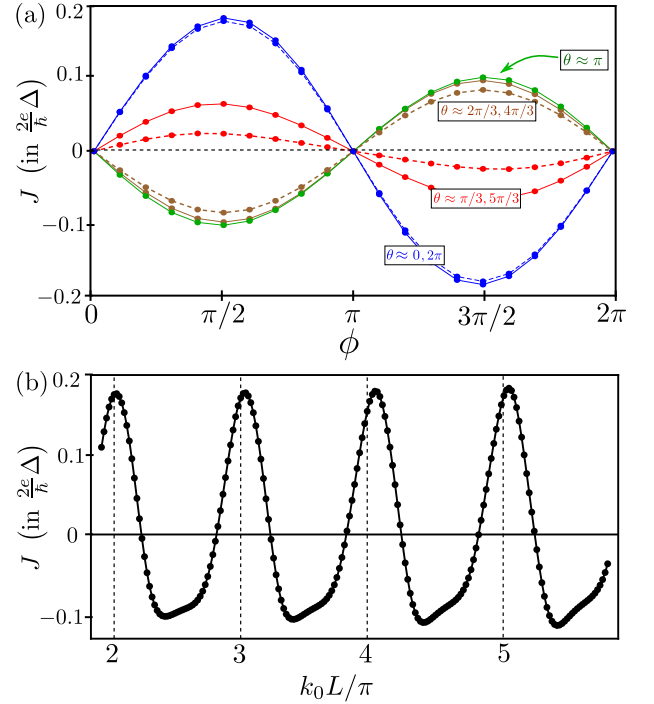

FIG. 5. (Color online) Result of lattice simulation: (a) Josephson current as a function of the superconducting phase difference ϕ for various values of $\theta = 2k_0 L \bmod(2\pi)$. (b) Josephson current as a function of the length $(k_0 L/\pi)$ at $\phi = \pi/2$. The parameters used are[43] $\tilde{t} = 0.25t$ (see Eq. (10)), $\epsilon = 6t$, $\lambda = \lambda_z = t$, $\Delta = 0.01t$, $\mu = 0.02t$ and $L = 60$ sites. For these parameters, the position of Weyl nodes, $k_0 = b_z/\lambda_z$ (the lattice constant is taken as the unit of length).

where ζ acts on the particle-hole degree of freedom in the Nambu basis and Σ_i is defined only on the sites in contact with the ith superconductor. $\tilde{t}$ characterises the tunnelling between the superconductor and the WSM[19]. Then writing the full Green's function as $G(\omega) = (g^{-1}(\omega) - \Sigma_L(\omega) - \Sigma_R(\omega))^{-1}$ we compute the Josephson current[43,50]. We find that the oscillations of current remain intact and this result has been summarized in Fig. 5. The bound levels E_b can also be found approximately for $p \ll k_0$ using Eq. (6), and the corresponding Josephson current also shows that the oscillation with $k_0 L$ remains intact[43].

Feasibility of experimental realization.—In the predicted WSM material TaAs[51,52], chiral node pairs (formed by breaking inversion symmetry) are separated in momentum space by a distance $\sim 0.02\text{Å}^{-1}$. Assuming standard electron mass, the relevant energy scale is about a milli electronvolt, which only becomes larger if the effective mass is smaller. Combining this with the fact that large momentum scattering (from $-k_0$ to k_0) is needed to break the topological protection of the chiral nodes, helical excitations in WSM are expected to be robust against disorder in a relatively clean sample. The periodicity of the Josephson current as well as the bound levels that we have discussed are, in principle, observable in tunneling

experiments. The periodic variation of the bound-levels can also be probed in Andreev spectroscopy. For a typical sample, the length scales for such periodic variations would be of the order of few tens of nanometers. The separation of the Weyl nodes can also be tuned by adjusting the magnetic doping[53–55] to observe periodicities with the separation of the Weyl nodes.

The effect of having many Weyl nodes complicates the theoretical modeling and presents a weakness in our proposal. But, as long as the transport takes place along a pair of Weyl nodes, a similar periodicity in the Josephson current is expected.

Summary and conclusion.—To summarize, we have shown explicitly, employing a simple model of the WSM, the occurrence of inter-nodal reflection processes at an WSM-SC interface due to spin conservation. This gives rise to an unusual periodicity in the bound state spectra

and consequently in the Josephson current that depends only on the separation of the two Weyl nodes and the size of the sample. This provides a direct path for possible observations of the manifestation of inter-nodal Andreev reflection in Weyl semimetals.

In closing, we sketch some problems for future studies. Apart from transport signatures of the chiral anomaly in WSM, the appearance of surface states, and the consequent Fermi arc dispersion is another remarkable feature of the time-reversal broken WSM. Their transport characteristics in the Josephson current would be interesting to study. Finally, quantitative investigations of the effects of disorder and interactions on transport in the WSM are also left for future studies.

[1] X. Wan, A. M. Turner, A. Vishwanath, S. Y. Savrasov, Phys. Rev. **B83**, 205101 (2011).

[2] A. A. Burkov and L. Balents, Phys. Rev. Lett. **107**, 127205 (2011).

[3] A. A. Burkov, M. D. Hook, and L. Balents, Phys. Rev. B **84**, 235126 (2011).

[4] A. A. Zyuzin, S. Wu, and A. A. Burkov, Phys. Rev. B **85**, 165110 (2012).

[5] P. Hosur, S. A. Parameswaran and A. Vishwanath, Phys. Rev. Lett. **108**, 046602 (2012).

[6] H. B. Nielsen and M. Ninomiya, Phys. Lett. B **105**, 219 (1981).

[7] A. M. Turner and A. Vishwanath, cond-mat/1301.0330

[8] S.-Y. Xu, I. Belopolski, N. Alidoust, M. Neupane, G. Bian, C. Zhang, R. Sankar, G. Chang, Z. Yuan, C.-C. Lee, S.-M. Huang, H. Zheng, J. Ma, D. S. Sanchez, B. Wang, A. Bansil, F. Chou, P. P. Shibayev, H. Lin, S. Jia, and M. Z. Hasan, Science **349**, 613 (2015).

[9] B. Q. Lv, H. M. Weng, B. B. Fu, X. P. Wang, H. Miao, J. Ma, P. Richard, X. C. Huang, L. X. Zhao, G. F. Chen, Z. Fang, X. Dai, T. Qian, and H. Ding, ArXiv e-prints (2015), 1502.04684.

[10] J. Y. Liu, J. Hu, D. Graf, S. M. A. Radmanesh, D. J. Adams, Y. L. Zhu, G. F. Chen, X. Liu, J. Wei, I. Chiorescu, L. Spinu, and Z. Q. Mao, ArXiv e-prints (2015), 1507.07978.

[11] S. Adler, Phys. Rev. **177**, 2426 (1969); J. S. Bell and R. Jackiw, Nuovo Cimento A **60**, 47 (1969)

[12] M. M. Vazifeh and M. Franz, Phys. Rev. Lett. **111**, 027201 (2013).

[13] O. Vafek and A. Vishwanath, Annual Review of Condensed Matter Physics **5**, 83 (2014).

[14] P. Hosur and X. Qi, Comptes Rendus Pysique, Vol. **14**, 857 (2013).

[15] W. Chen, L. Jiang, R. Shen, L. Sheng, B. G. Wang, and D. Y. Xing, Europhysics Letters **03**1, 27006 (2013).

[16] R. R. Biswas and Shinsei Ryu, Phys. Rev. B **89**, 014205 (2014).

[17] Y. Ominato and M. Koshino, Phys. Rev. B **89**, 054202 (2014).

[18] B. Sbierski, G. Pohl, E. J. Bergholtz and P. W. Brouwer,

[19] Phys. Rev. Lett. **113**, 026602 (2014).

[19] U. Khanna, A. Kundu, S. Pradhan and S. Rao, Phys. Rev. B **90**, 195430 (2014).

[20] A. A. Burkov, Journal of Physics: Condensed Matter **27**, 113201 (2015).

[21] D. T. Son and B. Z. Spivak, Phys. Rev. B **88**, 104412 (2013).

[22] A. A. Burkov, Phys. Rev. Lett. **113**, 247203 (2014).

[23] A. A. Burkov, Phys. Rev. B **91**, 245157 (2015).

[24] E. V. Gorbar, V. A. Miransky, and I. A. Shovkovy, Phys. Rev. B **89**, 085126 (2014).

[25] P. Goswami, J. H. Pixley, and S. Das Sarma, ArXiv e-prints (2015), 1503.02069.

[26] N. J. Ghimire, Y. Luo, M. Neupane, D. J. Williams, E. D. Bauer, and F. Ronning, Journal of Physics: Condensed Matter **27**, 152201 (2015).

[27] J. Klier, I. V. Gornyi, and A. D. Mirlin, ArXiv e-prints (2015), 1507.03481.

[28] A. A. Zyuzin and A. A. Burkov, Phys. Rev. B **86**, 115133 (2012).

[29] M. N. Chernodub, A. Cortijo, A. G. Grushin, K. Landsteiner, and M. A. H. Vozmediano, Phys. Rev. B **89**, 081407 (2014).

[30] A. Cortijo, Y. Ferreirós, K. Landsteiner, and M. A. H. Vozmediano, ArXiv e-prints (2015), 1506.05136.

[31] A. A. Burkov, J. Phys. Cond. Matt. **27**, 113201 (2015).

[32] Y. Baum, E. Berg, S. A. Parameswaran, and A. Stern, ArXiv e-prints (2015), 1508.03047.

[33] S. Uchida, T. Habe, and Y. Asano, J. Phys. Soc. Jpn. **83**, 064711 (2014).

[34] L. N. Bulaevski, V. V. Kuzii and A. A. Sobyanin, JETP Lett. **25**, 290 (1977).

[35] A. I. Buzdin, L. N. Bulaevski and S. V. Panyukov, JETP Lett. **35**, 178 (1982).

[36] A. I. Buzdin and M. Y. Kuprianov, JETP Lett. **53**, 308 (1991).

[37] For reviews, see A. A. Golubov, M. Y. Kupriyanov and E. Ilichev, Rev. Mod. Phys. 76, 411 (2004); A. I. Buzdin, Rev. Mod. Phys. 77, 935 (2005); F. S. Bergeret, A. F. Volkov and K. B. Efetov, Rev. Mod. Phys. 77, 1321 (2005).

[38] V. V. Ryazanov, V. A. Oboznov, A. Yu. Rusanov,

A. V. Veretennikov, A. A. Golubov, and J. Aarts, Phys. Rev. Lett. **86**, 2427 (2001).

[39] A. A. Golubov, M. Yu. Kuprianov and Ya. V. Fominov, JETP Lett. **75**, 190 (2002).

[40] T. Yokoyama, M. Eto, and Y. V. Nazarov, Phys. Rev. B **89**, 195407 (2014).

[41] X.-L. Qi and S.-C. Zhang, Rev. Mod. Phys. **83**, 1057 (2011)

[42] L. Fu and E. Berg, Phys. Rev. Lett. **105**, 097001, (2010)

[43] See the Supplemental material for details.

[44] O. Šipr and B. L. Györffy J. Low Temp. Phys. **106**, 315 (1997)

[45] L. Fu and C. L. Kane, Phys. Rev. Lett. **100**, 096407 (2008)

[46] A. Soori, O. Deb, K. Sengupta, and D. Sen, Phys. Rev. B **87**, 245435 (2013)

[47] C. W. J. Beenakker, Phys. Rev. Lett. **97**, 067007 (2006).

[48] A. Kundu, S. Rao, and A. Saha, Phys. Rev. B **82**, 155441 (2010).

[49] L.-F. Chang and P. F. Bagwell, Phys. Rev. B **55**, 12678 (1997).

[50] A. Martin-Rodero, F.J. Garcia-Vidal and A. Levy Yeyati, Phys. Rev. Lett. **72**, 554 (1994)

[51] S.-M. Huang, S.-Y. Xu, I. Belopolski, C.-C. Lee, G. Chang, B. Wang, N. Alidoust, G. Bian, M. Neupane, C. Zhang, S. Jia, A. Bansil, H. Lin, and M. Z. Hasan, Nature Communications **6**, 7373 (2015).

[52] L. X. Yang, Z. K. Liu, Y. Sun, H. Peng, H. F. Yang, T. Zhang, B. Zhou, Y. Zhang, Y. F. Guo, M. Rahn, D. Prabhakaran, Z. Hussain, S.-K. Mo, C. Felser, B. Yan, and Y. L. Chen, Nature Physics **11**, 728-732 (2015).

[53] Y. L. Chen, J.-H. Chu, J. G. Analytis, Z. K. Liu, K. Igarashi, H.-H. Kuo, X. L. Qi, S. K. Mo, R. G. Moore, D. H. Lu, M. Hashimoto, T. Sasagawa, S. C. Zhang, I. R. Fisher, Z. Hussain, and Z. X. Shen, Science **329**, 659 (2010)

[54] C.-Z. Chang, J.-S. Zhang, M.-H. Liu, Z.-C. Zhang, X. Feng, K. Li, L.-L. Wang, X. Chen, X. Dai, Z. Fang, X.-L. Qi, S.-C. Zhang, Y. Wang, K. He, X.-C. Ma, and Q.-K. Xue, Advanced Materials **25**, 1065-1070 (2013).

[55] D. Kurebayashi and K. Nomura, J. Phys. Soc. Jpn. **83**, 063709 (2014)